LETTER

doi:10.1038/nature10388

Antibiotic resistance is ancient

Vanessa M. D'Costa[1,2]*, Christine E. King[3,4]*, Lindsay Kalan[1,2], Mariya Morar[1,2], Wilson W. L. Sung[4], Carsten Schwarz[3], Duane Froese[5], Grant Zazula[6], Fabrice Calmels[5], Regis Debruyne[7], G. Brian Golding[4], Hendrik N. Poinar[1,3,4] & Gerard D. Wright[1,2]

The discovery of antibiotics more than 70 years ago initiated a period of drug innovation and implementation in human and animal health and agriculture. These discoveries were tempered in all cases by the emergence of resistant microbes[1,2]. This history has been interpreted to mean that antibiotic resistance in pathogenic bacteria is a modern phenomenon; this view is reinforced by the fact that collections of microbes that predate the antibiotic era are highly susceptible to antibiotics[3]. Here we report targeted metagenomic analyses of rigorously authenticated ancient DNA from 30,000-year-old Beringian permafrost sediments and the identification of a highly diverse collection of genes encoding resistance to β-lactam, tetracycline and glycopeptide antibiotics. Structure and function studies on the complete vancomycin resistance element VanA confirmed its similarity to modern variants. These results show conclusively that antibiotic resistance is a natural phenomenon that predates the modern selective pressure of clinical antibiotic use.

Recent studies of modern environmental and human commensal microbial genomes have a much larger concentration of antibiotic resistance genes than has been previously recognized[4–6]. In addition, metagenomic studies have revealed diverse homologues of known resistance genes broadly distributed across environmental locales. This widespread dissemination of antibiotic resistance elements is inconsistent with a hypothesis of contemporary emergence and instead suggests a richer natural history of resistance[2]. Indeed, estimates of the origin of natural product antibiotics range from 2 Gyr to 40 Myr ago[7,8], suggesting that resistance should be similarly old. Previous publications claim to have cultured resistant bacteria from Siberian permafrost (for example ref. 9), but these results remain contentious (see Supplementary Information).

To determine whether contemporary resistance elements are modern or whether they originated before our use of antibiotics, we analysed DNA sequences recovered from Late Pleistocene permafrost sediments. The samples were collected east of Dawson City, Yukon, at the Bear Creek (BC) site (Fig. 1); prominent forms of ground ice (ice wedges and surface icings) are preserved in the exposure, immediately overlain by a distinctive volcanic ash layer, the Dawson tephra[10,11] (Supplementary Table 1 and Supplementary Figs 1 and 2). The tephra has been dated at several sites in the area to about 25,300 radiocarbon (^{14}C) years BP, or about 30,000 calendar years[10,12]. The cryostratigraphic context is similar to other sites in the area preserving relict permafrost and indicates that the permafrost has not thawed since the time of deposition (Supplementary Information). In the absence of fluid leaching, the site represents an ideal source of uncontaminated and securely dated ancient DNA.

Two frozen sediment cores (BC1 and BC4), 10 cm apart, were obtained 50 cm below the tephra. In accordance with appropriate protocols[13], we monitored contamination introduced during coring by spraying the drilling equipment and the outer surface of the cores with high concentrations of *Escherichia coli* harbouring the *gfp* (green fluorescent protein) gene from *Aequorea victoria* (Supplementary Information).

After fracturing of the samples (Supplementary Fig. 3), total DNA was extracted from a series of five subsamples taken along the radius of each core (Supplementary Information). Quantitative polymerase

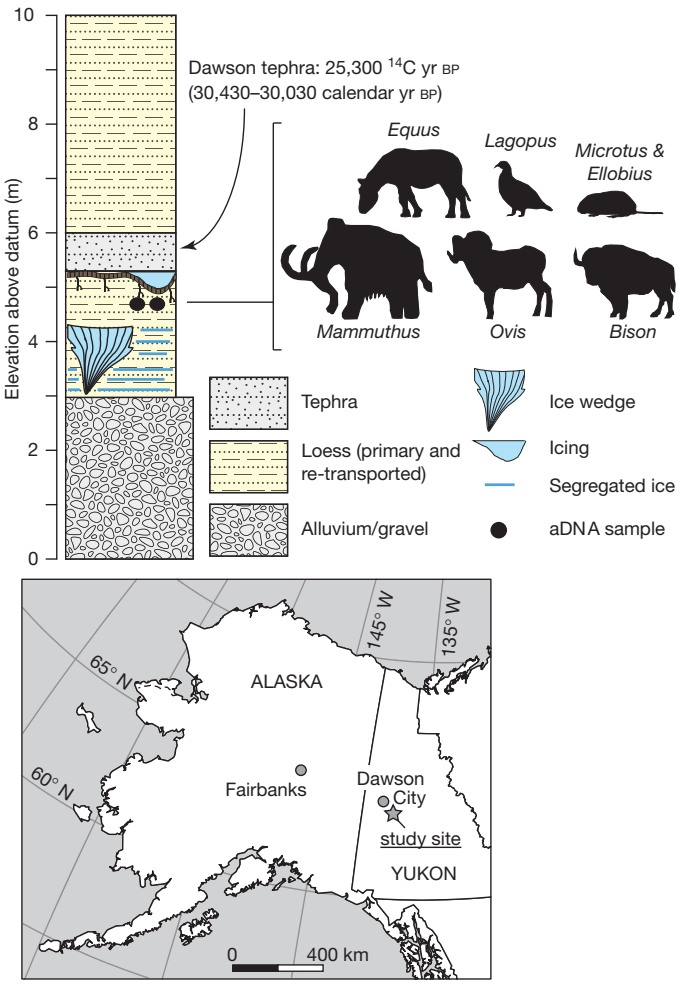

Figure 1 | Stratigraphic profile and location of Bear Creek site. Elevation is given in metres above base of exposure. Permafrost samples from below Dawson tephra were dated to about 30 kyr BP. Preservation of the ice below and above the sample indicates that the sediments have not thawed since deposition. Silhouettes represent mammals and birds identified from ancient DNA sequences that are typical of the regional Late Pleistocene environment. aDNA, ancient DNA.

[1]Michael G. DeGroote Institute for Infectious Disease Research, McMaster University, Hamilton, Ontario, Canada, L8N 3Z5. [2]Department of Biochemistry and Biomedical Sciences, McMaster University, Hamilton, Ontario, Canada, L8N 3Z5. [3]McMaster Ancient DNA Centre, Department of Anthropology, McMaster University, Hamilton, Ontario, Canada, L8S 4L9. [4]Department of Biology, McMaster University, Hamilton, Ontario, Canada, L8S 4K1. [5]Department of Earth and Atmospheric Sciences, University of Alberta, Edmonton, Alberta, Canada, T6G 2E3. [6]Yukon Palaeontology Program, Department of Tourism and Culture, Yukon Government, PO Box 2703, Whitehorse, Yukon, Canada, Y1A 2C6. [7]Muséum National d'Histoire Naturelle, UMR 7206 Eco-anthropologie, 57 rue Cuvier, CP139, 75231 Paris cedex 05, France.

*These authors contributed equally to this work.

chain reaction (qPCR) analysis confirmed extremely high yields of *gfp* on both core exteriors, with 0.1% or less of this amount at the centre (Supplementary Information and Supplementary Fig. 4). This supports negligible leaching or cross-contamination during subsampling.

A crucial step lending support for the authenticity of the ancient DNA was to confirm the presence of DNA derived from flora and fauna characteristic of a late Pleistocene age, and the absence of common modern or Holocene floral and faunal sources. To explore the vertebrate and plant diversity, we amplified fragments of the mitochondrial 12S rRNA and chloroplast *trn*L and *rbc*L genes (Supplementary Table 3). Amplicons were sequenced with the 454 GS-FLX platform and identified by BLAST analysis of GenBank sequences (Supplementary Information).

The vertebrate sequences included abundant Late Pleistocene megafauna such as *Bison*, *Equus* and *Ovis*, as well as rodents (*Microtus* and *Ellobius*) and the rock ptarmigan, *Lagopus mutus* (Supplementary Fig. 6 and Supplementary Table 5). *Mammuthus* was detectable at low copy numbers with the use of a mammoth-specific qPCR assay, which is consistent with the low ratio of these fossils relative to bison and horse in the region[11,14]. The *rbc*L and *trn*L sequences revealed many plant groups that are also well documented in Beringia, including the grasses *Poa* and *Festuca*, sage (*Artemisia*) and willow (*Salix*)[15] (Supplementary Figs 7 and 8, and Supplementary Tables 6 and 7). No sequences of common Holocene vertebrates (for example elk or moose) or plants (for example spruce) were identified despite sequence conservation across the primer-binding sites; these results are consistent with other reports[16] that have argued against DNA leaching in permafrost sediments.

We focused our investigation of bacterial 16S rRNA sequences on the Actinobacteria, known for their ability to synthesize diverse secondary metabolites and for harbouring antibiotic resistance genes[4]. Deep sequencing of 16S amplicons (Supplementary Information) revealed genera commonly found in soil and permafrost microbial communities[17], including *Aeromicrobium*, *Arthrobacter* and *Frankia* (Supplementary Fig. 9 and Supplementary Table 8). Analysis of contaminant 16S sequences derived from extraction and PCR control reactions (Supplementary Table 4) suggested that these do not contribute to the ancient DNA data set; in fact not only were the copy numbers 1,000–30,000-fold lower than from the permafrost extracts, but with the exception of unclassified bacteria there was also very little overlap in the genera identified (Supplementary Fig. 9 and Supplementary Table 8). Querying the permafrost sequences against the contaminant data set with the use of BLAST further confirmed their disparity: only 1% of the reads had 95–100% identity to a contaminant sequence, with a single sequence showing 100% identity.

We next developed a series of assays to detect genes encoding resistance to several major classes of antibiotic and representing diverse strategies of drug evasion (for example target modification, target protection and enzymatic drug inactivation) (Supplementary Information). Determinants included the ribosomal protection protein TetM, which confers resistance to tetracycline antibiotics by weakening the interaction between the drug and the ribosome; the D-Ala-D-Ala dipeptide hydrolase VanX, which is a component of the vancomycin resistance operon; the aminoglycoside-antibiotic-modifying acetyltransferase AAC(3); a penicillin-inactivating β-lactamase Bla (a member of the TEM group of β-lactamases); and the ribosome methyltransferase Erm, which blocks the binding of macrolide, lincosamide and type B streptogramin antibiotics. Amplification of *vanX*, *tetM* and *bla* fragments was successful, and triplicate PCR products from multiple extracts were cloned and multiple clones were sequenced.

The β-lactamase sequences demonstrated amino-acid identities between 53% and 84% with known determinants and clustered with one of two groups of enzymes: characterized β-lactamases from streptomycetes and uncharacterized β-lactamase-like hydrolytic proteins (Fig. 2a and Supplementary Fig. 14). We identified several *tetM*-related genes in the permafrost, most of which were most closely related to the actinomycete subset of ribosomal protection proteins, including the biochemically characterized self-resistance element OtrA from the oxytetracycline producer *Streptomyces rimosus*[18] (Fig. 2b). Most intriguing was the identification of *vanX* gene fragments, which spanned the entire phylogenetic space of characterized vancomycin resistance determinants found in the clinic and in the environment. These branch away from the cellular dipeptidases that are the likely progenitors the *vanX* family (Supplementary Fig. 10).

Vancomycin resistance took the clinical community by surprise when it emerged in pathogenic enterococci in the late 1980s[19]. In both clinical pathogens[19] and contemporary soil environments[4], resistance results from the acquisition of a three-gene operon *vanH–vanA–vanX* (*vanHAX*). These enzymes collectively reconstruct bacterial peptidoglycan to terminate in D-alanine-D-lactate in place of the canonical D-alanine-D-alanine, which is required for vancomycin binding and

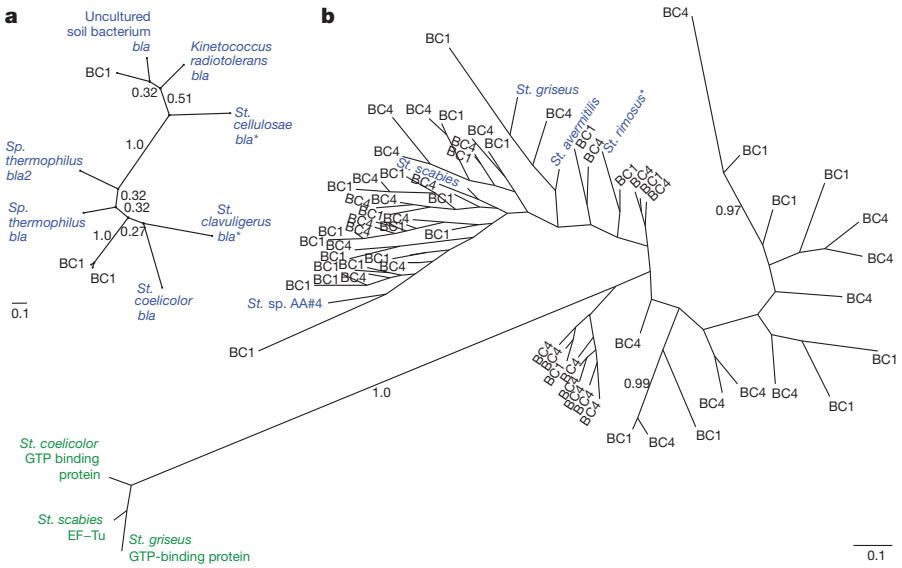

Figure 2 | Genetic diversity of ancient antibiotic resistance elements. **a**, **b**, Unrooted Bayesian phylogenies of translated β-lactamase (*bla*) (**a**) and tetracycline resistance (*tetM*) (**b**). Blue denotes predicted resistance enzymes, and green those associated with other functions; permafrost-derived sequences are labelled with the originating core name. Sequences in which resistance activity has been biochemically verified are noted with a single asterisk (Supplementary Information). The scale bar represents 0.1 substitutions per site. Posterior probabilities are shown for **a**, and those of 0.7 or more are indicated for **b**. All unlabelled tips derive from ancient sequences. BC1, Bear Creek sample 1; BC4, Bear Creek sample 4.

subsequent antibiotic action. Although most forms of resistance are attributed to a single gene, this complex mechanism is exclusively associated with resistance and thus its presence provides unambiguous confirmation of its role as a resistance determinant.

With few exceptions, the *vanHAX* operon is invariant in genetic organization; it therefore offers a matchless template for confirming its presence with PCR assays that span the *vanHA* and *vanAX* boundaries. Two short qPCR assays were designed to confirm this contiguity

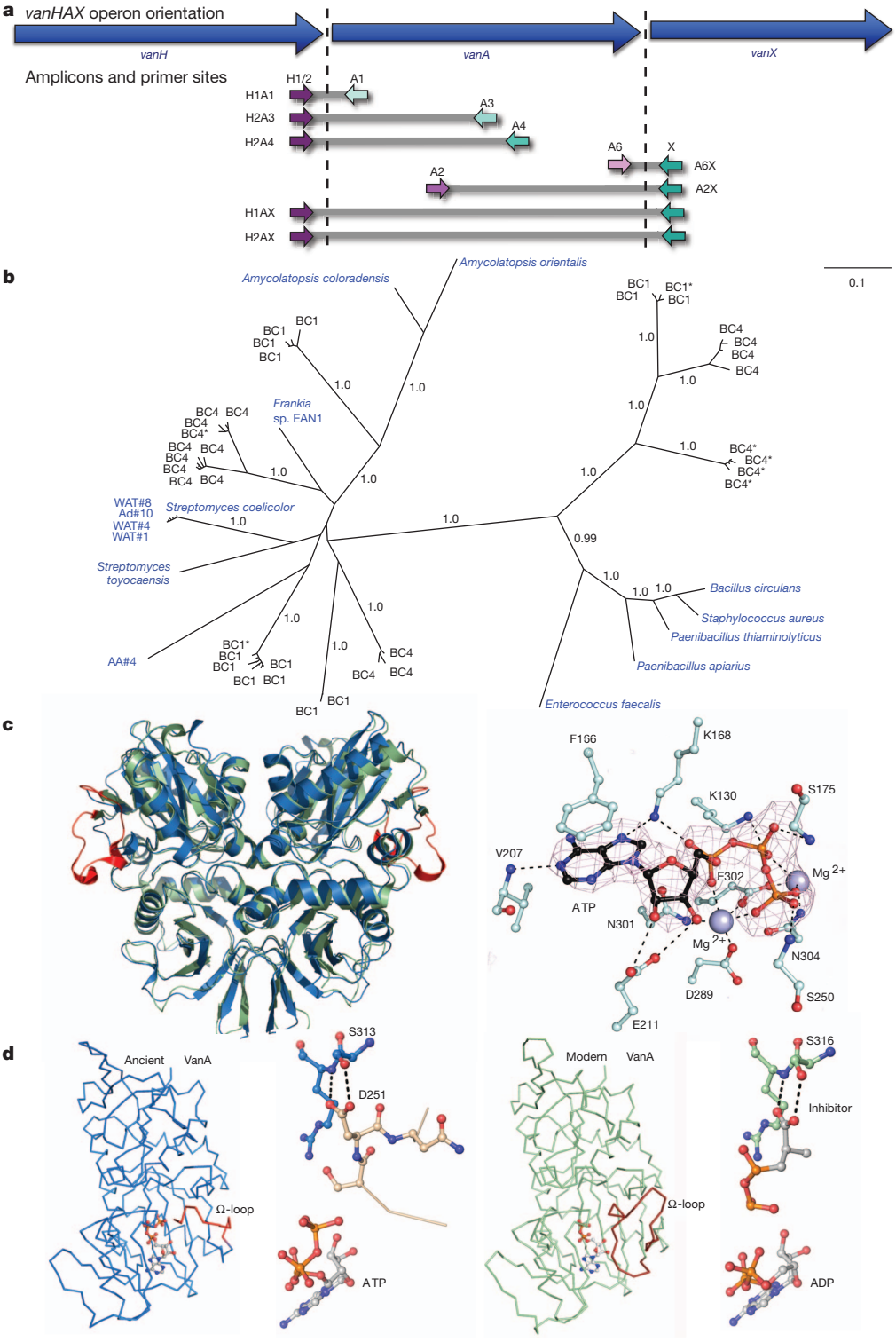

Figure 3 | Ancient vancomycin resistance elements. **a**, *vanHAX* amplicons used in this study, with primer names noted above each arrow. **b**, Unrooted Bayesian phylogeny of translated *vanA* sequences; blue denotes strains with *vanHAX* clusters confirmed to confer resistance; sequences containing stop codons but homology throughout are noted with a single asterisk (Supplementary Information). BC1, Bear Creek sample 1; BC4, Bear Creek sample 4. **c**, $VanA_{A2}$ structure. Left: ribbon diagram of the $VanA_{A2}$ dimer (blue) overlaid with modern VanA (green), where the Ω-loop is coloured red; right: ball-and-stick representation of ATP binding. The electron density shown is an $F_o - F_c$ map contoured at 3σ. **d**, Comparison of modern and ancient VanA monomer structures. The Ω-loop is coloured red and detailed in the ball-and-stick figures. Ligands are shown in grey. Dashed lines represent hydrogen bonds.

Table 1 | *vanHAX* permutation tests

Amplicon	Number	Length (base pairs)	Probability of similarity by chance alone to *Streptomyces coelicolor genes*		
			vanH	*vanA*	*vanX*
H1A1	164	203–213	3.59×10^{-3}	4.39×10^{-17}	0.24
H1A1*	12	209–216	2.83×10^{-3}	8.16×10^{-16}	0.28
H2A3	24	573–605	9.83×10^{-3}	1.27×10^{-54}	0.22
H2A4	79	666–681	4.33×10^{-3}	6.15×10^{-53}	0.18
A6X	159	170–179	0.11	6.87×10^{-8}	5.64×10^{-9}
A6X*	11	176–179	0.04	2.96×10^{-8}	3.63×10^{-9}
A2X	96	735–796	0.11	1.80×10^{-59}	1.35×10^{-6}
HAX†	40	1,173–1,204	5.95×10^{-3}	9.32×10^{-92}	6.47×10^{-7}

* Clones from independent replication in France. †Includes both H1AX and H2AX.

(Fig. 3a and Supplementary Information). Positive results, including particularly high yields of the smallest amplicon, A6X (Supplementary Table 9), encouraged us to attempt amplification across both boundaries (that is, the complete *vanA* gene) in a single 1.2-kilobase amplicon. We also targeted fragments anchored on either boundary and extending as far as possible into *vanA*. None of the sequences from these products, or those generated by an independent laboratory (Supplementary Information), were present in GenBank. No contaminants were detected in more than 300 control reactions.

Phylogenetic analyses showed that many of the ancient *vanHAX* sequences cluster with characterized glycopeptide-resistant strains of Actinobacteria containing *vanHAX* cassettes (for example streptomycetes, glycopeptide-producing *Amycolatopsis* species and the nitrogen-fixing *Frankia* sp. EAN1pec) (Fig. 3b and Supplementary Figs 11 and 12). Another group falls between the actinobacterial sequences and the Firmicutes-derived cluster, which includes environmental *Paenibacillus* isolates and the pathogenic *Enterococci*, and may reflect an intermediate group.

Permutation tests were performed with the PRSS algorithm[20] (1,000 permutations each) to confirm that the sequences were statistically similar to those of vancomycin resistance genes (*vanHAX*) present in modern *Streptomyces*. As shown in Table 1, all *vanHA*-spanning clones have significant similarity to *vanH* and *vanA*, and all *vanAX*-spanning clones have significant similarity to *vanA* and *vanX*.

To ascertain whether the complete *vanA* sequences are indeed functional and do not represent PCR artefacts or pseudogenes, we synthesized four open reading frames from the 40 H1AX/H2AX sequences (Supplementary Information). Two of these generated soluble proteins suitable for purification to homogeneity. Enzymatic characterization indicated that these ligases were indeed D-alanine-D-lactate-specific (Supplementary Fig. 13), and analysis revealed steady-state kinetic parameters consistent with contemporary enzymes derived from both the clinic and the environment (Supplementary Table 10). These results clearly show that the *vanHAX* genes identified in the ancient samples encode enzymes capable of genuine antibiotic resistance.

We further confirmed the link between 30,000-year-old VanA and contemporary enzymes by determining the three-dimensional structure of $VanA_{A2}$ by X-ray crystallography (Supplementary Table 11 and Supplementary Information). The quaternary and tertiary structures of $VanA_{A2}$, crystallized in the ATP-bound form, show the overall D-Ala-D-X ligase fold of modern enzymes including VanA from vancomycin-resistant *Enterococcus faecium* (Fig. 3c, d). Superposition of ancient and modern VanA (Fig. 3c, d) reveals conservation of quaternary and tertiary structure with minor differences in Mg^{2+} and ATP γ-phosphate coordination. The Ω-loop comprises the biggest structural change; 13 amino-terminal residues (233–246) are absent from the electron density map of $VanA_{A2}$, including His 241 (His 244 in modern VanA), responsible for the lactate selectivity. The last seven Ω-loop residues (247–253) have clear electron density, undergoing a drastic 13 Å shift. These structural differences, however, are not reflected in enzyme function.

This work firmly establishes that antibiotic resistance genes predate our use of antibiotics and offers the first direct evidence that antibiotic resistance is an ancient, naturally occurring phenomenon widespread in the environment. This is consistent with the rapid emergence of resistance in the clinic and predicts that new antibiotics will select for pre-existing resistance determinants that have been circulating within the microbial pangenome for millennia. This reality must be a guiding principle in our stewardship of existing and new antibiotics.

METHODS SUMMARY

Permafrost cores were collected at Bear Creek, Yukon, then shipped frozen to the McMaster Ancient DNA Centre and stored at −40 °C. All subsequent procedures before PCR/qPCR amplification were performed in dedicated clean rooms, physically separated from laboratories containing modern DNA, bacterial cultures and amplification products. Contaminant leaching into the centre of cores after sampling was monitored by qPCR assays designed to detect *E. coli* DNA encoding the jellyfish green fluorescent protein sprayed onto coring equipment and the external surfaces of all collected cores. DNA was extracted from the centre of subsampled permafrost cores. PCR assays were designed to target vertebrates, plants, bacteria and specific antibiotic resistance elements. All products were sequenced with either the 454 GS-FLX platform or by standard cloning and sequencing procedures (GenBank accession numbers JN316287–JN366376). The ancient *vanA* gene identified from the permafrost was synthesized and expressed in *E. coli*, and the His_6-tagged protein was purified by immobilized metal-affinity chromatography. This protein was used in enzymatic studies to determine steady-state kinetics and was also studied by crystallography using the vapour-diffusion hanging-drop method. Data were collected at the National Synchrotron Light Source, Brookhaven National Laboratory, beamline X25 (PDB 1E4E).

Received 28 March; accepted 22 July 2011.
Published online 31 August 2011.

1. Livermore, D. M. Has the era of untreatable infections arrived? *J. Antimicrob. Chemother.* **64,** i29–i36 (2009).
2. Wright, G. D. The antibiotic resistome: the nexus of chemical and genetic diversity. *Nature Rev. Microbiol.* **5,** 175–186 (2007).
3. Hughes, V. M. & Datta, N. Conjugative plasmids in bacteria of the 'pre-antibiotic' era. *Nature* **302,** 725–726 (1983).
4. D'Costa, V. M., McGrann, K. M., Hughes, D. W. & Wright, G. D. Sampling the antibiotic resistome. *Science* **311,** 374–377 (2006).
5. Dantas, G., Sommer, M. O. A., Oluwasegun, R. D. & Church, G. M. Bacteria subsisting on antibiotics. *Science* **320,** 100–103 (2008).
6. Sommer, M. O. A., Dantas, G. & Church, G. M. Functional characterization of the antibiotic resistance reservoir in the human microflora. *Science* **325,** 1128–1131 (2009).
7. Baltz, R. H. Antibiotic discovery from actinomycetes: will a renaissance follow the decline and fall? *SIM News* **55,** 186–196 (2005).
8. Hall, B. G. & Barlow, M. Evolution of the serine β-lactamases: past, present and future. *Drug Resist. Updat.* **7,** 111–123 (2004).
9. Mindlin, S. Z., Soina, V. S., Petrova, M. A. & Gorlenko, Z. M. Isolation of antibiotic resistance bacterial strains from Eastern Siberia permafrost sediments. *Russ. J. Genet.* **44,** 27–34 (2008).
10. Froese, D. G., Zazula, G. D. & Reyes, A. V. Seasonality of the late Pleistocene Dawson tephra and exceptional preservation of a buried riparian surface in central Yukon Territory, Canada. *Quat. Sci. Rev.* **25,** 1542–1551 (2006).
11. Froese, D. G. *et al.* The Klondike goldfields and Pleistocene environments of Beringia. *GSA Today* **19,** 4–10 (2009).
12. Brock, F., Froese, D. G. & Roberts, R. G. Low temperature (LT) combustion of sediments does not necessarily provide accurate radiocarbon ages for site chronology. *Quat. Geochronol.* **5,** 625–630 (2010).
13. Willerslev, E., Hansen, A. J. & Poinar, H. N. Isolation of nucleic acids and cultures from fossil ice and permafrost. *Trends Ecol. Evol.* **19,** 141–147 (2004).
14. Harington, C. R. & Clulow, F. V. Pleistocene mammals from Gold Run Creek, Yukon Territory. *Can. J. Earth Sci.* **10,** 697–759 (1973).
15. Zazula, G. D. *et al.* Ice-age steppe vegetation in east Beringia. *Nature* **423,** 603 (2003).

16. Haile, J. *et al.* Ancient DNA reveals late survival of mammoth and horse in interior Alaska. *Proc. Natl Acad. Sci. USA* **106,** 22352–22357 (2009).
17. Gilichinsky, D. *et al.* in *Psychrophiles: From Biodiversity to Biotechnology* (eds Margesin, R., Schinner, F., Marx, J.-C. & Gerday, C.) 83–102 (Springer, 2008).
18. Doyle, D., McDowall, K. J., Butler, M. J. & Hunter, I. S. Characterization of an oxytetracycline-resistance gene, *otrA*, of *Streptomyces rimosus*. *Mol. Microbiol.* **5,** 2923–2933 (1991).
19. Courvalin, P. Vancomycin resistance in gram-positive cocci. *Clin. Infect. Dis.* **42,** S25–S34 (2006).
20. Pearson, W. R. & Lipman, D. J. Improved tools for biological sequence comparison. *Proc. Natl Acad. Sci. USA* **85,** 2444–2448 (1988).

Supplementary Information is linked to the online version of the paper at www.nature.com/nature.

Acknowledgements We thank A. Guarné for assistance in X-ray data collection. This work was supported by Canada Research Chairs to D.F., H.N.P. and G.D.W., a Canadian Institutes of Health Research operating grant to G.D.W. (MOP-79488) and a scholarship to V.M.D., and by grants from the Natural Sciences and Engineering Research Council of Canada to D.F. and H.N.P. and scholarship to C.E.K.

Author Contributions D.F., G.Z. and F.C. collected permafrost cores and performed geochemical analyses followed by subsampling by C.S., V.M.D. and C.E.K. C.E.K performed ancient DNA laboratory work and 454 sequencing. V.M.D. designed primers for resistance genes, 16S and *gfp*. V.M.D. and C.E.K. designed and optimized the qPCR assays, and cloned and sequenced the resistance gene products. R.D. independently confirmed the results in France. L.K. purified and characterized VanA, and M.M. crystallized VanA and determined the three-dimensional structure. W.S., G.B.G., C.E.K. and H.N.P. processed and analysed the floral/faunal data; V.M.D. and G.B.G. performed phylogenetic and bioinformatic analyses of the resistance gene sequences. H.N.P. and G.D.W. conceived the project, and V.M.D., C.E.K., D.F., H.N.P. and G.D.W. wrote the manuscript. All authors edited the final draft.

Author Information The metagenomic sequences determined from permafrost are deposited in GenBank under accession numbers JN316287–JN366376. Reprints and permissions information is available at www.nature.com/reprints. The authors declare no competing financial interests. Readers are welcome to comment on the online version of this article at www.nature.com/nature. Correspondence and requests for materials should be addressed to G.D.W. (wrightge@mcmaster.ca) or H.N.P. (poinarh@mcmaster.ca).